

# Breathing Thorax Simulation based on Pleura Physiology and Rib Kinematics

Anne-Laure Didier<sup>1</sup>, Pierre-Frédéric Villard<sup>1</sup>, Jean-Yves Bayle<sup>2</sup>,  
Michaël Beuve<sup>1</sup>, Behzad Shariat<sup>1</sup>

<sup>1</sup> Université de Lyon, Lyon, F-69003, France ; université Lyon 1, CNRS UMR5205,  
LIRIS, Villeurbanne, F-69622, France

<sup>2</sup> Hôpital Louis Pradel, Lyon, France  
{anne-laure.didier, pierre-frederic.villard}@liris.univ-lyon1.fr

## Abstract

*To monitor a lung mechanical model and then predict tumour motion we proposed a approach based on the pleura physiology. By comparing the predictions to landmarks set by medical experts, we observed better results with regards to the one obtained with approaches found in the literature. Beside, we focus on the rib cage kinematics, which play a significant role in the pleura outer-surface motion and therefore in the lung motion. We proposed a kinematic model of the rib cage based on the finite helical axis method and we show out interesting results.*

**Keywords**—Finite Element Method, Dynamic Deformable Model, Thorax Physiology, Rib Cage Kinematics

## 1 Introduction

During a radiotherapy treatment, healthy tissues have to be preserved while the dose has to be concentrated on the tumour. These goals are especially difficult to achieve with pulmonary tumour due to patient's breathing. Hence, the knowledge of lung-tumor positions during any step of breathing cycle would dramatically improve lung cancer treatment.

We developed a lung numerical model to estimate such a motion. This model is based on the continuous mechanics laws, which are solved with the finite element method. Our results leaded to compute the displacement of every point inside the lung with only knowing lung surface motion.

Our strategy is now to monitor our simulation with lung external surface. Therefore, we will provide in a first section some elements lung physiological and lung environment. We will especially focus on the pleura, the rib cage and the diaphragm because they play a significant role on lung-surface motion. This information is essential to understand our approach, which is strongly based on medical reality. In a second section we will then explain how our model considers the pleura physiology and we will propose a clinical evaluation. Finally, a motion model of the

rib cage is presented in the last section.

## 2 Respiratory Physiology

Respiration is a complex mechanical process, which mobilises many elements we describe below.

### 2.1 The lung

Lungs take up most of the thorax volume. The left lung is smaller due to the space occupied by the heart. The two lungs are separated by the mediastinum, which contains the heart, important arteries, veins, trachea, oesophagus and lymph gland. During breathing, the lungs keep contact with the rib cage and the diaphragm through the pleura and follow any of their motions.

### 2.2 The pleura

The pleura is composed of two membranes: the first called parietal covers the chest wall, mediastinum and diaphragm while the second is called visceral and covers the outer surface of the lungs. The space in between, known as the pleural space, is filled with an incompressible pleural fluid. The surface tension of this fluid enables the contact between lung surface on one hand, and, the rib cage and the diaphragm on the other hand. This fluid lubricates the pleural surfaces and allows the lungs to easily slide against the chest wall when they expand. During inhalation, the motion of the diaphragm and of the rib cage induces a negative pressure (with regards to atmospheric pressure) in the pleural cavity leading to a tensile stress on the lungs.

### 2.3 Rib cage and intercostal muscles

The rib cage is composed of the sternum, twelve rib pairs, costal cartilage and twelve thoracic vertebrae. The first seven ribs, called true ribs, are linked directly to the sternum (by their own costal cartilage) while the height to ten ribs joined the seventh rib by their costal cartilage. The last two ribs, called false ribs, are not link to the sternum and have not costal cartilage. All ribs are connected to spine and are more or less inclined astern. The Thorax has

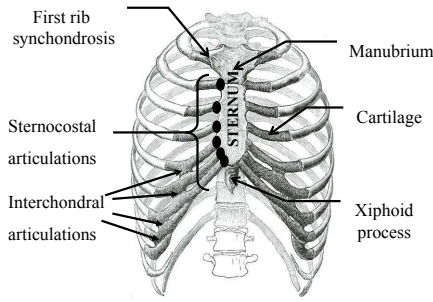


**Figure 1. rib articulations**

a lot of articulations and we will enlighten: 1- the sternocostal (between the cartilage and the sternum), 2-the interchondral (cartilage between themselves), and 3- the costovertebral (synovial joint between ribs and vertebrae).

We can assimilate the rib motion to a “bucket handle” movement mixed with a “pump handle” one. We can note that the upper ribs have a more pronounced “pump handle” movement than the lower ribs for which “bucket handle” is sharper. Rib motion is led by the intercostal muscles, which stand between the ribs. Internal intercostal muscles are only activated during forced exhalation (quiet exhalation is a passive process). External intercostal muscles (EIM) are relatively important in both quiet and forced inhalation. EIM insert into ribs 2-12 and are responsible for ribs elevation and Postero-Anterior thoracic diameter raising.

## 2.4 The diaphragm

The most important muscle of the respiration is the diaphragm. Our final aim is to include this muscle in our numerical model. It is a digastric muscle that separates the thoracic cavity from the abdominal one. It is made of two domes: the right comes up on the fourth intercostal space whereas the left does not go past the fifth one. The diaphragm is constituted by a peripheral part (muscular fibers) and by a central tendon. Its peripheral part is linked with the whole lower thoracic cavity perimeter and has three major insertions: lumbar, sternum and ribs.

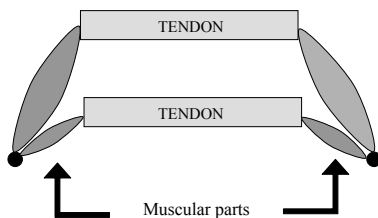


**Figure 2. diaphragm motion simplification**

During inspiration, the contraction of muscular fibers brings down the central tendon (figure 2). This lowering increases the vertical diameter of the thorax. There are many inspiration accessory muscles like scalenes or sternocleidomastoid but they do play a role only for high ventilation that is out of our application field.

## 3 Pleura Influence Modeling

In the literature, many methods were studied to model the behaviour of thorax system. But only two classes of methods focus on lungs: 1 - The discrete methods consist in discretising the organ into mass points and in applying interaction laws in between ([8], [12] and [9]) 2 - The continuous methods, consist in defining every mechanical quantities as continuous function inside the whole organ. Continuous approach seems more adapted to model lungs within the accuracy required by our radiotherapy context: they generally use continuous mechanics principles but few of them focus on respiration modelling. We note that these latter models do not take into account the pleura influence. For instance, in [3], boundary conditions are set by the displacements determined from a non-rigid registration. In [2], Brock *et al.* simulate lung inflation by imposing orthogonal displacements to its surface (Cf Figure 3, left). In terms of mechanics, this **OD** method (**OD** for **O**rthogonal **D**isplacements) consists in assuming that inhalation is only produced by the negative pressure of the respiration muscles. Hence, each lung-surface point follows a displacement perpendicular to the lung surface. In [10], we defined boundary conditions that explicitly take into account the pleura influence as described in §2.2. Here, We propose to compare the results obtained for both approaches in order to show the importance of the pleura role.

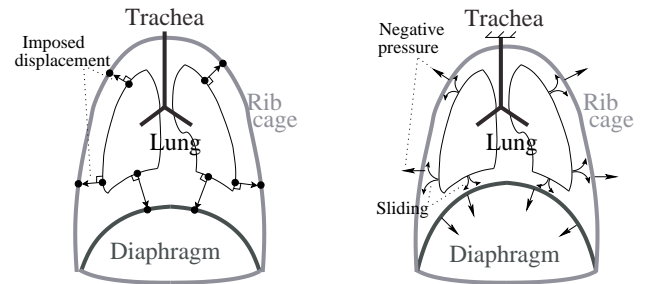


**Figure 3. Boundary conditions apply to lungs: left: OD method and right: Our method**

### 3.1 Our model

Our model is based on continuous mechanics laws. We consider lung tissue as homogeneous, isotropic, and its constitutive equation defined by a linear elastic behaviour.

Moreover, we assume that normal breathing can be approximated by a series of quasi-static states. Our boundary conditions are illustrated on Figure 3, *right*. Lungs are fixed near the trachea, and the pleura behaviour is simulated by applying contact conditions allowing lung surface to slide against pleura. The contact conditions model the negative intra-pleural pressure and the sliding surface models the lubricating fluid inside pleural cavity (Cf §2.2). At the same time, the inflation from an initial state to a final state is caused by a negative pressure applied to lung surface. This models the muscle actions.

The system with these three kinds of equations (constitutive, dynamics and boundary conditions) is solved with the finite element method. We use Code-Aster [1], a finite element software developed by the French Electricity Board (EDF) for the last 20 years. The required computing time is then 10 times more important than with the OD method. This is due to the non-linearity of the system (contact conditions). In principle the results obtained with our model should be in better agreement with reality because it includes a more realistic description of anatomy. However we verified this assumption by a clinical comparisons of both methods.

### 3.2 Clinical comparison

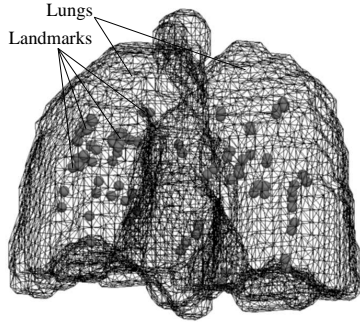


**Figure 4. Example of landmark positions inside Patient 2's lungs. Each landmark has been determined by medical experts.**

To compare both methods we defined a validation protocol. We considered two sequences of 4D CT scan (one for Patient1 and one for Patient2) acquired according to a protocol similar to the one described in [7]. On each sequence, we selected four levels of lung inflation. This allows to define three transitions that is to say three pairs of initial and final states. We assumed that real motion data could be estimated by a series of "landmarks" determined by three medical experts. Example of landmark positions could be seen on Figure 4.

We proceed now to the simulation of these three lung motions using first the OD method and then our own

method. Orthogonal displacements are defined on each mesh vertex and are computed with the ray-triangle intersection method presented in [6].

We defined for both models the same mesh, composed of 30000 elements, and the same computer, a Pentium 4, 2.40GH with 1GB memory. Finally, only the boundary conditions were different. We gather the simulation results on Table 1 for Patient 1 and Table 2 for Patient 2. For each selected points, we calculated the differences between the simulated displacements and the landmark displacements (reference values). Histograms of errors can be found on Table 1 and Table 2. OD average error amounts to 3.1mm for Patient 1 and to 6.16mm for Patient 2, while the same error with our method amounts to 2.14mm for patient 1 and to 5.16mm for patient 2.

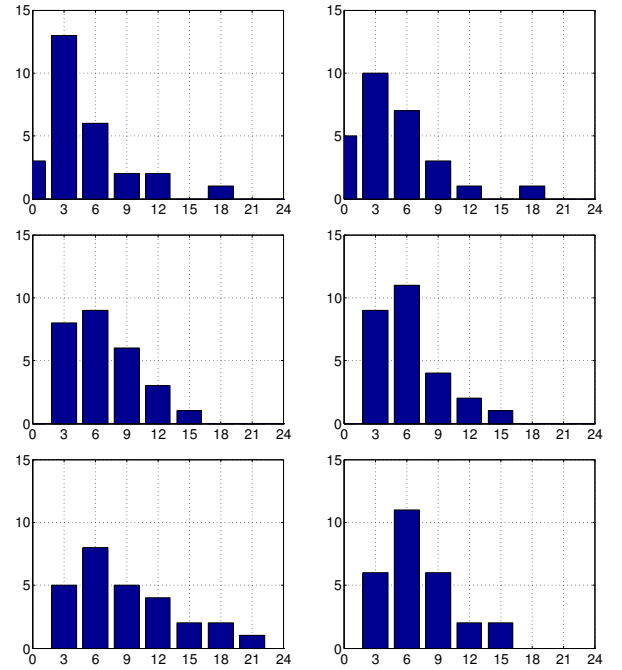


**Table 1. Patient 1 histograms of displacement errors such as  $error = |position_{simulation} - position_{experts}|$ . X axis represents the intervals of displacement errors (in mm) and the number of such errors. From top to bottom the three levels of inflation and Left: OD method, right: Our method**

### 3.3 Discussion on pleura influence

Tables 1 and 2 show that pleura influences lung behaviour. Indeed, not only it shows that simulations from both methods lead to different results but also that taking into account the pleura sliding gives results in better agree-

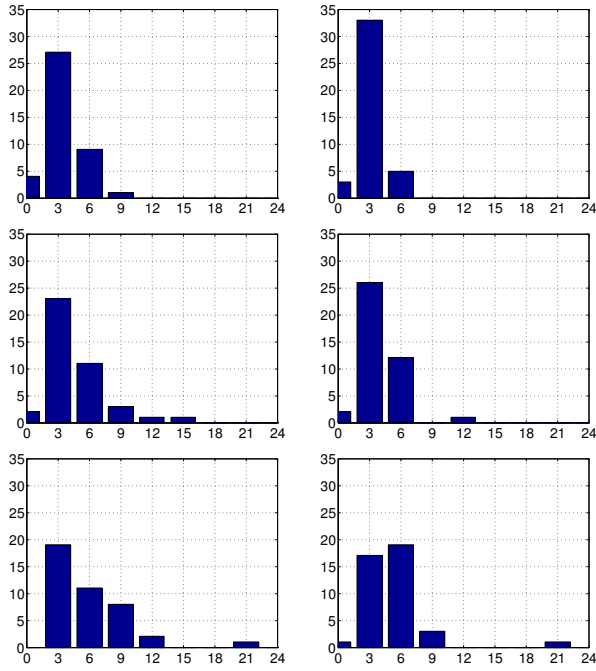


**Table 2. Patient 2 histograms of displacement errors such as  $error = |position_{simulation} - position_{experts}|$ . X axis represents the intervals of displacement errors (in mm) and the number of such errors. From top to bottom the three levels of inflation and Left: OD method, right: Our method**

ment with clinical data. For both patients, histograms with our method have more bins corresponding to small errors. The average error is also less important with our method than with the **OD** method. In particular, we note that the lateral displacement is underestimated with **OD** approach.

For both methods majority of displacement errors remains below 1cm which is better than actual routine method consisting in ignoring the displacements. Nevertheless, results could be improved. Mesh resolution is only 10cm<sup>3</sup>. Besides, landmarks were chosen by experts on strong heterogeneity area (carina, calcified nodules, culmen-lingula junction, division branch of pulmonary artery, apical pulmonary vein of upper lobe, etc), where displacement errors are expected more important because of the assumption of homogeneous mechanical properties. Finally, dynamic simulation of lung behaviour will be more accurate by taking pleura influence into account.

## 4 Control of the pleura outer-surface motions

As mentioned in section §2, the pleura and therefore the lung motion are monitored by the diaphragm and the rib cage. In this section, we propose a kinematics model of the rib cage. By the past, few authors took an interest in the rib kinematics like T.A.Wilson [11] who studied the displacement of human ribs and defined their rotation axis with a system of rib planes. To obtain rib shape and magnitude of displacements in **all** directions, we chose another method called the finite helical axis method.

### 4.1 Finite Helical Axis Method

The FHA method is often applied to describe a rigid body displacement between two successive states. The aim of the FHA method is to describe a solid movement by a rotation and a translation around and along an axis. The principles of this method are illustrated in the Figure 5, where  $X_i, Y_i, Z_i$  is a coordinate system linked to a solid at an initial state and  $X_f, Y_f, Z_f$  is the same coordinate system after transformation.

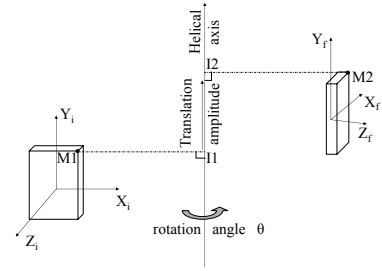


**Figure 5. Finite helical axis method principle**

To get the FHA parameters of ribs, we worked only on their solid parts (Cf section §2) and we used the relative rotation operator (Equation 1).

$$\begin{pmatrix} c\theta + kx^2(1 - c\theta) & kxky(1 - c\theta) - kzs\theta & kys\theta + kxkz(1 - c\theta) \\ kzs\theta + kxky(1 - c\theta) & c\theta + ky^2(1 - c\theta) & -kxs\theta + kykz(1 - c\theta) \\ -kys\theta + kxkz(1 - c\theta) & kxs\theta + kykz(1 - c\theta) & c\theta + kz^2(1 - c\theta) \end{pmatrix} = [a]_{ij} \quad (1)$$

where  $c\theta = \cos \theta$ ,  $s\theta = \sin \theta$ ,  $kx, ky, kz$  : axis direction

Chèze et al. [4] applied it, with markers glued on the skin, and noted that the inaccuracy in the measurement leads to errors in the position and direction of the FHA. Spoor and al. [5] showed that these measurement errors cause a result error inversely proportional to the rotation magnitude. They insisted on the fact that a high degree of measurement accuracy of marker coordinates is required for reasonably accurate of the direction and position of the

axis. In our study, we extracted from CT-scan anatomical point landmarks, which is unmistakably a more precise method than markers. To get the FHA parameters, the displacement and orientation changes of a coordinate system attached to the rib through respiration-cycle time are required. This system is built from three non-aligned rib points (one near the rib head, another on the middle and the last just before the cartilage part). These point positions are identified on the scans at each breathing level. So, we obtain the coordinate-system position attached to a rib at the initial state and at the final state. By applying the equation (1), we acquire the rotation angle, the FHA direction and orientation, the translation amplitude by using the relations described in [4].

The aim of our work is to predict, from the rotation parameters, the rib positions at any time. Therefore, we applied Rodrigues formula, which reads in the case of an helical displacement (Cf Figure 5):

$$M_1 \vec{M}_2 = 2\vec{k} \tan \frac{\theta}{2} \times \left( \frac{I_1 \vec{M}_1 + I_2 \vec{M}_2}{2} \right) + I_1 \vec{I}_2 \quad (2)$$

To verify the performance of our proposal, at the initial state (end of exhalation), we chose ten points placed on the seventh rib midline illustrated on Figure 6. We plotted them on the thorax which has been segmented from the initial scan. We applied our method and we obtained these point positions at the final state (Figure 7).

We proposed a linear interpolation of the transformation to predict the rib motion at any intermediate breathing states as follows:

$$\begin{aligned} \theta &= x\theta_{max} \\ t &= xT_{max} \end{aligned} \quad (3)$$

Where  $x \in [0, 1]$  is the interpolation coefficient,  $\theta_{max}$  and  $T_{max}$  are respectively the rotation angle and the translation amplitude between exhalation end and inhalation end. To evaluate the validity of our interpolation, we compute the rib points for  $x=0.5$  (which is certainly the most penalizing for our algorithm) and compared them to the position of the seventh rib at the intermediate breathing level (Figure 8).

#### 4.2 Firsts Results

We defined some reference-point positions at the end of exhalation as the rib midline (cf. Figure 6). The reference points were linked in order to enhance visualization.

We computed, by using the Rodrigues Formula (Equation 2), the positions of these reference points at the final state (end of inhalation). The results are illustrated on Figure 7.

We observe that the predicted final points match well with the rib midline. We observed this agreement whatever the visualization directions is.

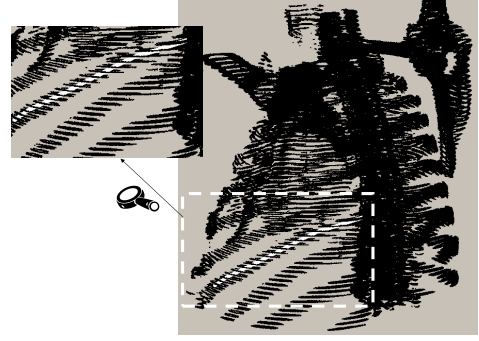


**Figure 6. Profile of segmented thorax: definition of the reference points at the initial state (in white)**



**Figure 7. Simulation of the reference points at the final state (in white)**

We evaluated our interpolation method for the case (Equation 3)  $x=0.5$  by comparing our predictions to the seventh rib on the segmented thorax at the intermediate breathing level.

Our computed final-points are very close to the rib midline points, so, we can conclude that the rib motion can be well interpolated with our method.

To evaluate the robustness of our method, we estimated the error generated by the uncertainty in setting the point coordinates of the coordinate systems attached to the rib.

As expected, the error in Figure 9 is more important than in Figure 7 but it is still acceptable and the data remain workable.

#### Conclusion

In this work we focused on the monitoring of lung mechanical models to simulate motions during breathing. We first showed that taking into account the pleura physiology gives predictions in better agreement with clinical data with regard to the results of mechanical model proposed in the literature. Since the external surface of pleura follows the rib cage, we secondly proposed a FHA model of rib cage kinematics that predicts the rib position at any time. The only required input is the manual registration





**Figure 8. Interpolation method: simulation of reference points at the intermediate state (in white)**



**Figure 9. Simulation of the reference point positions at the final state (in white)**

of 3 non-aligned rib points for one breathing state to another. The first results are promising. Beside we numerically evaluated the sensibility of our approach to the accuracy of the landmark-points setting and we concluded to a rather correct robustness of our method. Actually, the landmark points are chosen manually, but we plan to explore deformable-registration techniques to reduce man/machine interactions. The complete monitoring of the lung motion will be achieved after modeling of diaphragm motion with the help of additional data such as the patient air-breath rate.

## 5 Acknowledgements

We thank the French league against cancer for their financial support and all our partners: Léon Bérard Centre and ETOILE<sup>1</sup> Center for their support.

## References

- [1] Code Aster. <http://www.code-aster.org/>.

<sup>1</sup><http://etoile.in2p3.fr>

- [2] K.K. Brock, M.B. Sharpe, L.A. Dawson, S.M. Kim, and D.A. Jaffray. Accuracy of finite element model-based multi-organ deformable image registration. *Medical physics*, 32(6):1647–59, June 2005.
- [3] Y. Chi, J. Liang, and D. Yan. A material sensitivity study on the accuracy of deformable organ registration using linear biomechanical models. *Medical physics*, 33(2):421–433, February 2006.
- [4] L. Chèze, B.J. Fregly, and J. Dimnet. Determination of joint functional axes from noisy marker data using the finite helical axis. *Human Movement Science*, 17:1–15, 1998.
- [5] C.W.Spoor. Explanation, verification and application of helical-axis error propagation formulas. *Human Movement Science*, pages 95–117, 1984.
- [6] T. Möller and B. Trumbore. Fast, minimum storage ray-triangle intersection. *journal of graphics tools*, 2(1):21–28, 1997.
- [7] T. Pan, T.Y. Lee, E. Rietzel, and G.T.Chen. 4D-CT imaging of a volume influenced by respiratory motion on multi-slice CT. *Medical physics*, 31(2):333–340, 2004.
- [8] A.P. Santhanam, C.M. Fidopiastis, F.G. Hamza-Lup, J.P. Rolland, and C.Imielinska. Physically-based deformation of high-resolution 3d lung models for augmented reality based medical visualization. In *MIC-CAI AMI-ARCS*, pages 21–32., 2004.
- [9] P.W. Segar, D.S. Lalush, and B.M.W. Tsui. Modeling respiratory mechanics in the mcat and spline-based mcat phantoms. *IEEE Transactions on Nuclear Science*, I(48):89–97, 2001.
- [10] P-F. Villard, M. Beuve, B. Shariat, V. Baudet, and F. Jaillet. Simulation of lung behaviour with finite elements : Influence of bio-mechanical parameters. *IEEE, Mediviz, Conference on Information Visualization*, pages 9–14, 2005.
- [11] T. A. Wilson, K. Rehder, S. Kraye, E. A. Hoffman, C. G. Whitney, and J. R. Rodarte. Geometry and respiratory displacement of human ribs. *Journal of Applied Physiology*, 62(5):1872–1877, 1987.
- [12] V.B. Zordan, B. Celly, B. Chiu, and P.C. DiLorenzo. Breathe easy : Model and control of simulated respiration for animation. *ACM SIGGRAPH Symposium on Computer Animation*, 2004.